

PIC simulation study of the parametric instabilities of Alfvén-ion-cyclotron waves and their turbulence in a low beta plasma

*Chang-Mo RYU,
Helen H. KAANG, Kicheol RHA*

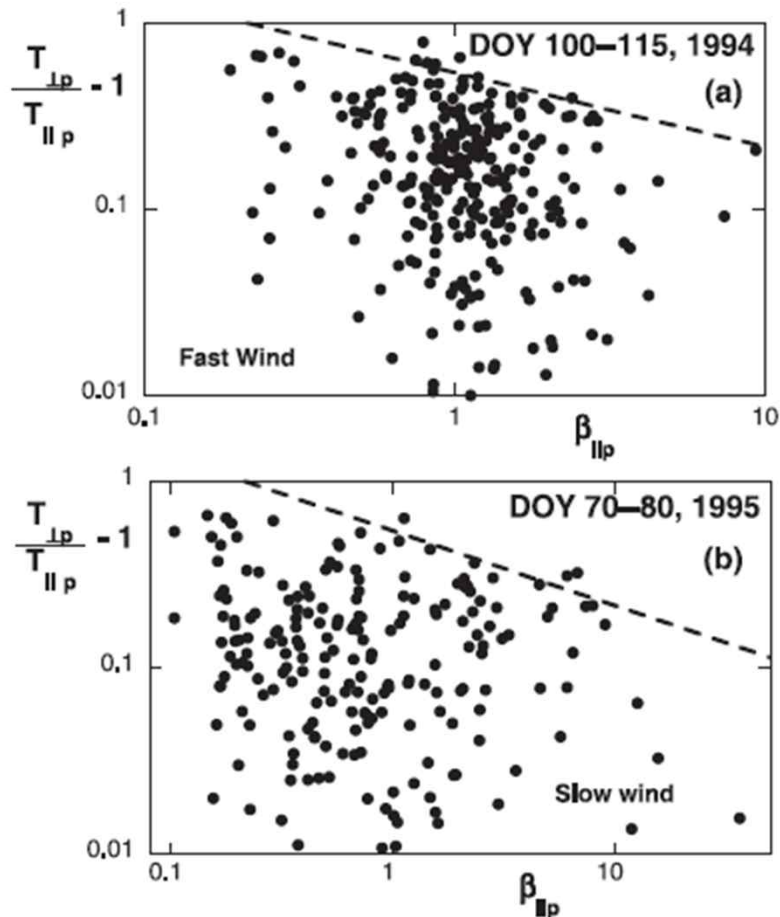
POSTECH

2011.11

Outline

1. Introduction
 - Space observation
2. Simulation Results
 - with Initially imposing Alfvénic perturbation
 - with anisotropic temperature
3. Summary

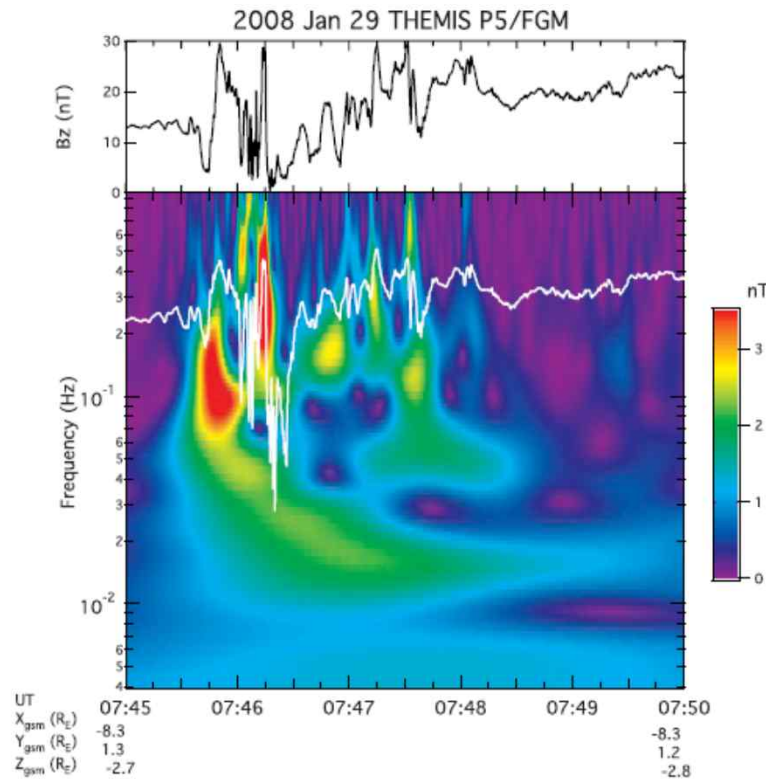
EMIC Instability in Solar Wind



Temperature anisotropy in the solar wind (Ulysses data analyses). [Gary et al., JGR(2009)]

- $T_{\perp i}/T_{\parallel i} > 1$ [Marsch et. al, 1982; Neugebauer et al.,2001;Gary et al. 2002]
- ⇒ Electromagnetic ion-cyclotron (EMIC) instability can be excited
 - Anisotropic ion kinetic energy with ambient magnetic field
- EMIC mode is observed in space.

EMIC Turbulence in Magnetotail

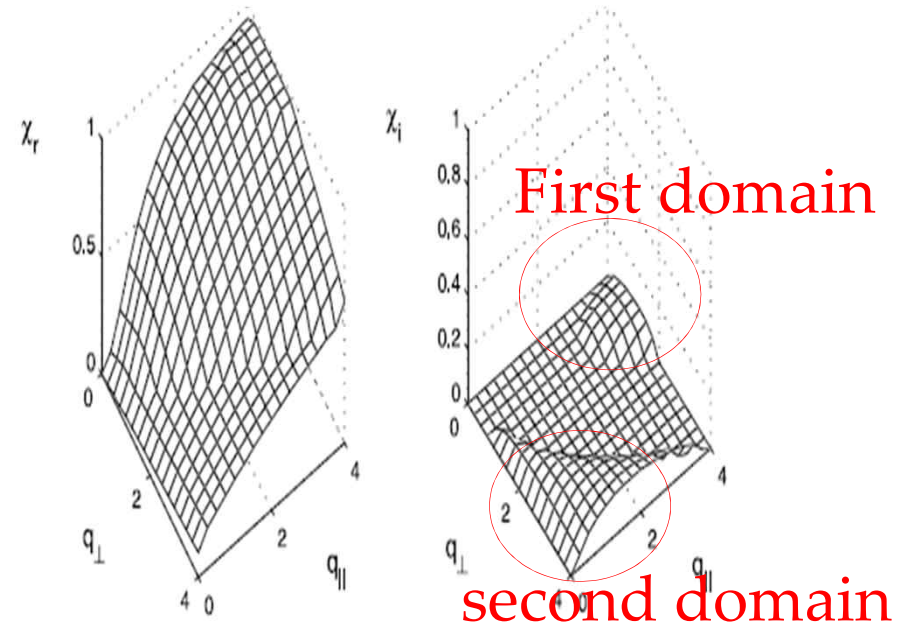


Wavelet analysis of observation data by THEMIS satellite [Lui et al., JGR(2008)].

- Turbulence observed in the magnetotail.
- The inverse cascade begins at high frequencies and settles at low frequencies.
- EMIC instability occurs in two distinct frequency domains.
- These instabilities can be explained by EMIC modes induced by ion drift.

EMIC Instability Induced by Ion Drift

- The wave spectrum is characterized by a gap between the two unstable modes.
- EMIC instability occurs in two distinct frequency domains.
- The first domain corresponds to waves propagating nearly along the magnetic field.
- The second regime corresponds to waves propagating mainly perpendicular to the magnetic field.



The linear dispersion curve of the EMIC instability induced by ion drift [Mok et al., JGR(2010)].

Excitation of EMIC waves in simulation

Two methods to excite Alfvén-ion-cyclotron waves:

- Initially imposing Alfvénic perturbation : using Walén condition

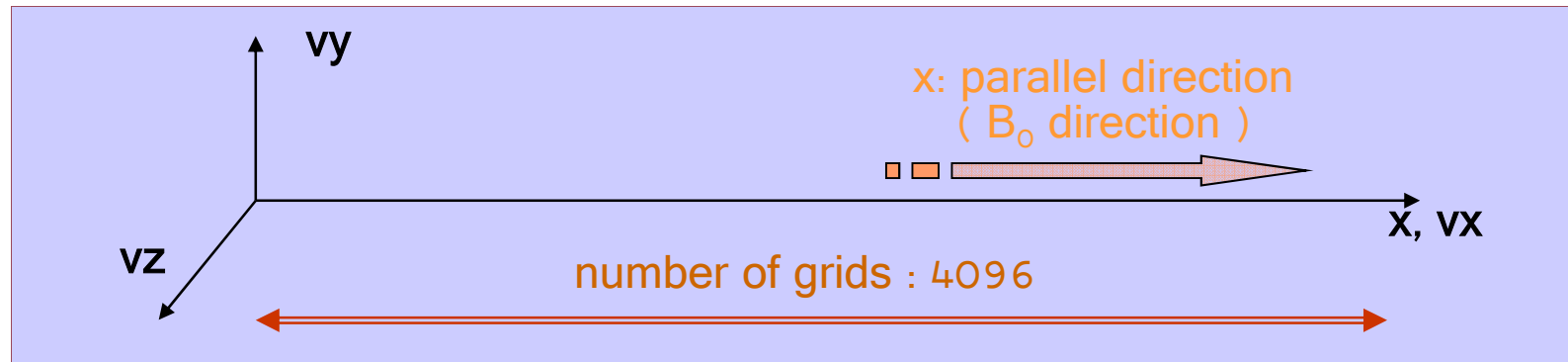
$$b_p = \sum_{k_0=k_1}^{k_2} b_{k_0}^h \exp[i(\omega_0 t - k_0 x + \phi_{k_0})],$$

$$v_p = \sum_{k_0=k_1}^{k_2} v_{k_0}^h \exp[i(\omega_0 t - k_0 x + \phi_{k_0})], \quad \text{where, } k_0^2 = \frac{\omega_0^2}{1 \pm \omega_0}$$

- Anisotropic temperature

1D PIC Simulation with Alfvénic Perturbation

Initially imposed Alfvénic perturbation with isotropic temperature plasma



- $m_i/m_e = 16$
- Strength of the background magnetic field : $\Omega_e/\omega_{pe} = 0.5$
- Initial temperature(isotropic Maxwellian distribution)
: $\beta_e = 0.08, \beta_i = 0.1$
- Number of particles : 4000/cell for each species

Initially Imposed Alfvenic Perturbation

$$\delta B(x, t = 0) = \sum_{n=1}^{15} \{ \delta B_{L_n} [\cos(k_{L_n} x) \hat{y} + \sin(k_{L_n} x) \hat{z}] + \delta B_{R_n} [\cos(k_{R_n} x) \hat{y} - \sin(k_{R_n} x) \hat{z}] \}$$

$$\left(\frac{\delta B_{L(R)_n}}{B_0} \right)^2 = w_0 \exp \left(-\frac{\kappa_{L(R)_n}^2}{\Delta^2} \right), \quad w_0 = 1 \text{ and } \Delta = 0.25.$$

$$\kappa_{L(R)_n} = \frac{k_{L(R)_n} v_A}{\Omega_i} \quad \text{and} \quad \omega_{L_n} = \frac{k_{L_n} v_A}{\sqrt{1 + k_{L_n}^2 v_A^2 / \Omega_i^2}},$$

$$\omega_{R_n} = k_{R_n} v_A \sqrt{1 + \frac{k_{R_n}^2 v_A^2}{\Omega_i^2}}.$$

Table 1. Parameters for fluctuation spectrum.

n	$\kappa_{L(R)_n}$	ω_{L_n} / Ω_i	ω_{R_n} / Ω_i
1	0.798	0.624	1.02
2	0.828	0.638	1.08
\vdots	\vdots	\vdots	\vdots
15	1.23	0.775	1.94

* k : positive

$$\delta v_i = \sum_{n=1}^{15} \left\{ \frac{\delta B_{L_n}}{B_0} [\cos(k_{L_n} x) \hat{y} + \sin(k_{L_n} x) \hat{z}] \times \left(\frac{(\omega_{L_n} - \Omega_c)(\omega_{L_n}^2 - c^2 k_{L_n}^2)}{(\omega_{pc}^2 + \omega_{pi}^2) k_{L_n}} - \frac{\omega_{L_n}}{k_{L_n}} \right) \right.$$

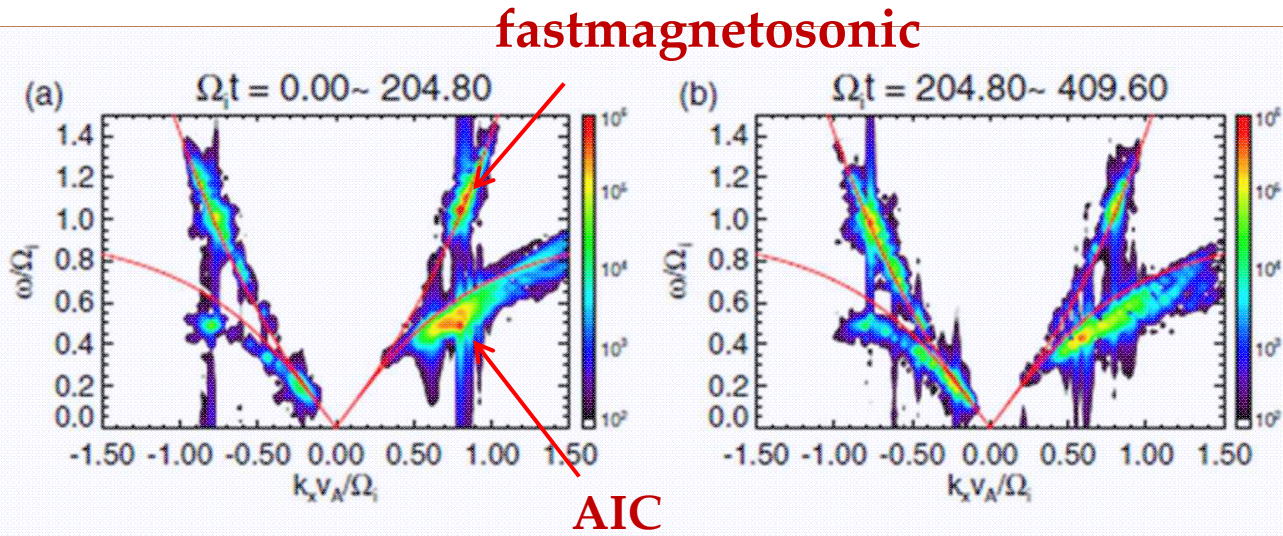
$$\left. + \frac{\delta B_{R_n}}{B_0} [\cos(k_{R_n} x) \hat{y} - \sin(k_{R_n} x) \hat{z}] \times \left(\frac{(\omega_{R_n} + \Omega_c)(\omega_{R_n}^2 - c^2 k_{R_n}^2)}{(\omega_{pc}^2 + \omega_{pi}^2) k_{R_n}} - \frac{\omega_{R_n}}{k_{R_n}} \right) \right\},$$

$$\delta v_c = \sum_{n=1}^{15} \left\{ \frac{\delta B_{L_n}}{B_0} [\cos(k_{L_n} x) \hat{y} + \sin(k_{L_n} x) \hat{z}] \times \left(\frac{(\omega_{L_n} - \Omega_i)(\omega_{L_n}^2 - c^2 k_{L_n}^2)}{(\omega_{pc}^2 + \omega_{pi}^2) k_{L_n}} - \frac{\omega_{L_n}}{k_{L_n}} \right) \right.$$

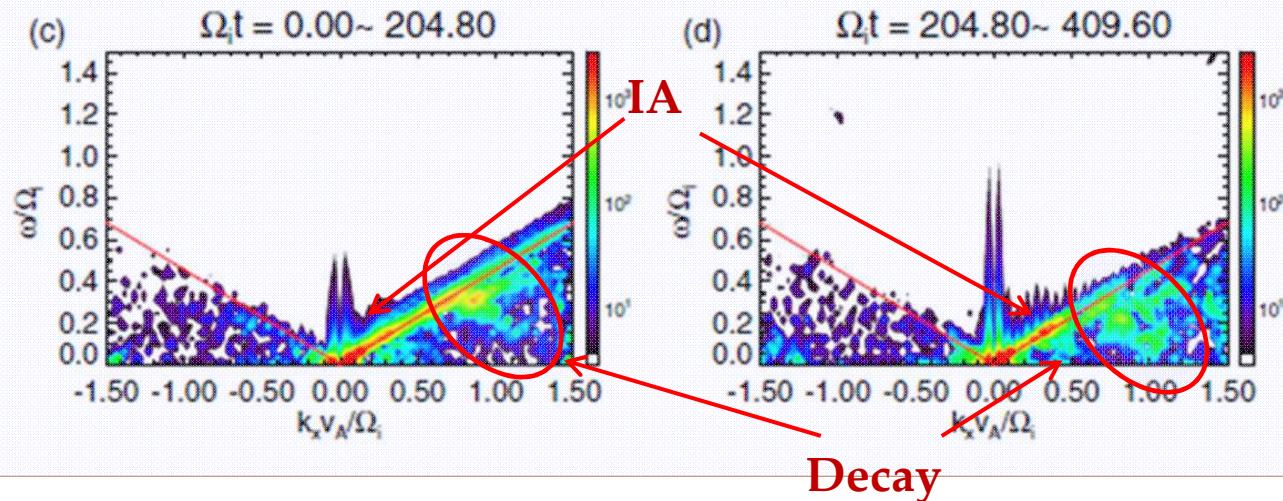
$$\left. + \frac{\delta B_{R_n}}{B_0} [\cos(k_{R_n} x) \hat{y} - \sin(k_{R_n} x) \hat{z}] \times \left(\frac{(\omega_{R_n} + \Omega_i)(\omega_{R_n}^2 - c^2 k_{R_n}^2)}{(\omega_{pc}^2 + \omega_{pi}^2) k_{R_n}} - \frac{\omega_{R_n}}{k_{R_n}} \right) \right\}.$$

Alfven-cyclotron & fast-magnetosonic waves

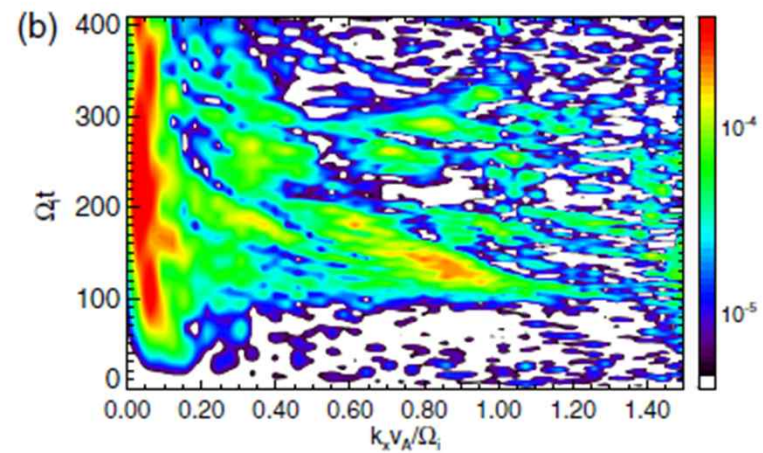
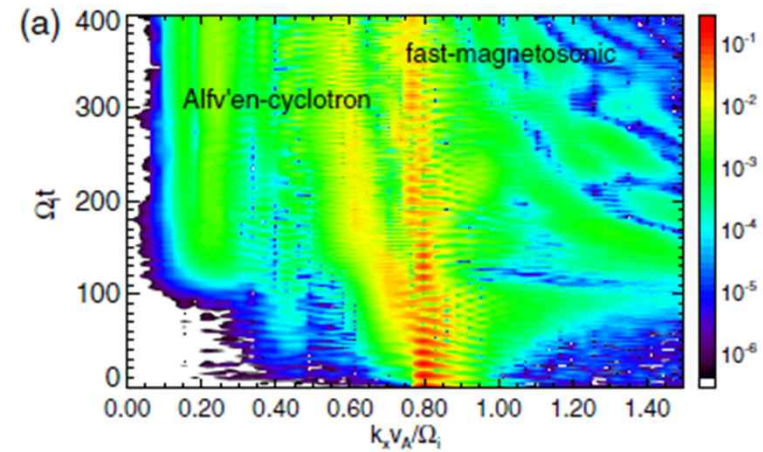
ω -k
of B_z



ω -k
of n_i

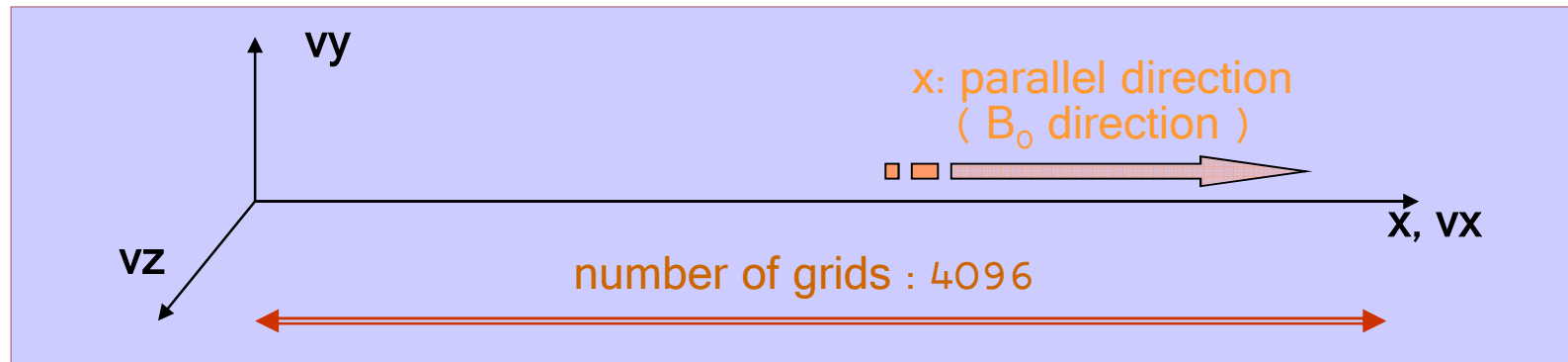


Time Evolution of Excited Modes



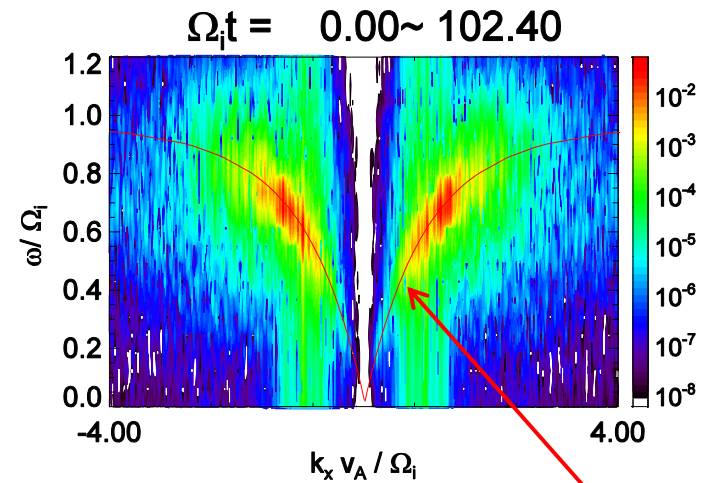
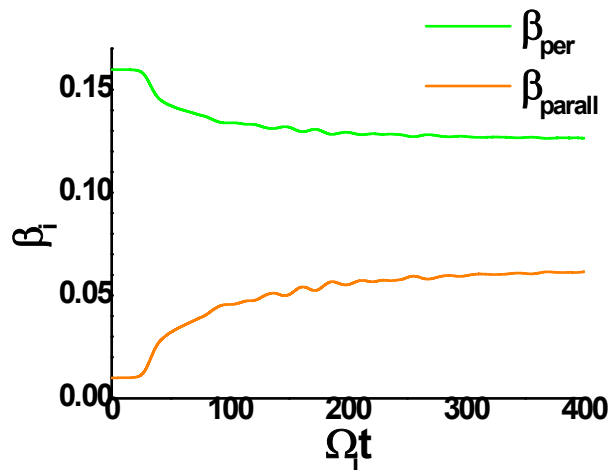
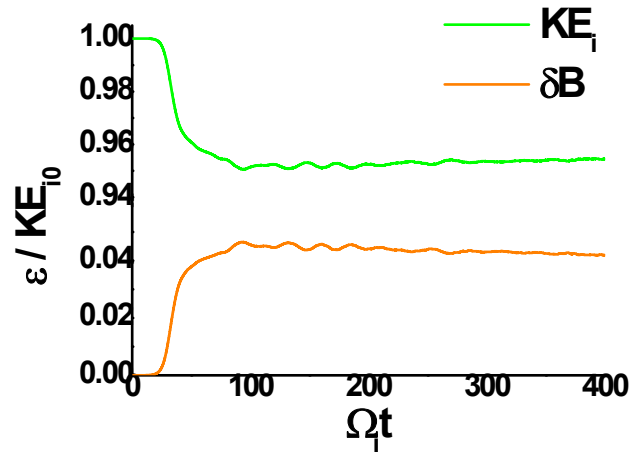
1D PIC Simulation with Anisotropic T

Magnetized plasma with anisotropic ion temperature.



- $m_i/m_e = 25$
- Strength of the background magnetic field : $\Omega_e/\omega_{pe} = 0.5$
- Initial temperature(with Maxwellian distribution)
 - electron (isotropic) : $\beta_e = 0.04$
 - ion (anisotropic) : $\beta_{\perp i} = 0.16$, $\beta_{\parallel i} = 0.01$
- Number of particles : 4000/cell for each species

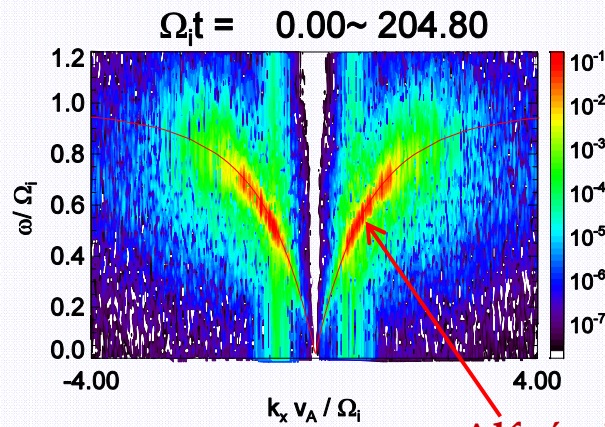
Energy & Temperature, Excited AIC Mode



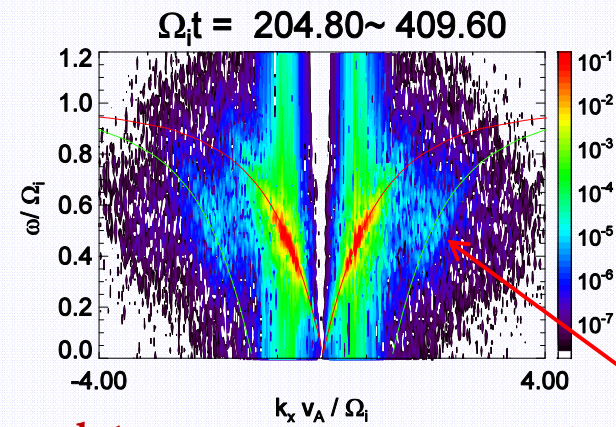
Alfvén-ion-cyclotron (AIC) dispersion curve

Excited Modes at Different Times

ω - k
of B_z

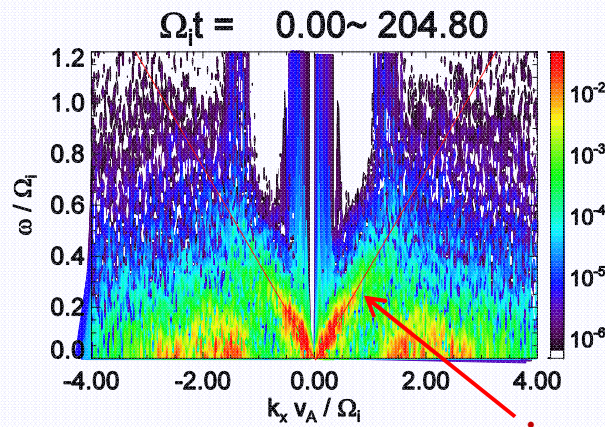


Alfvén-ion-cyclotron
(AIC)

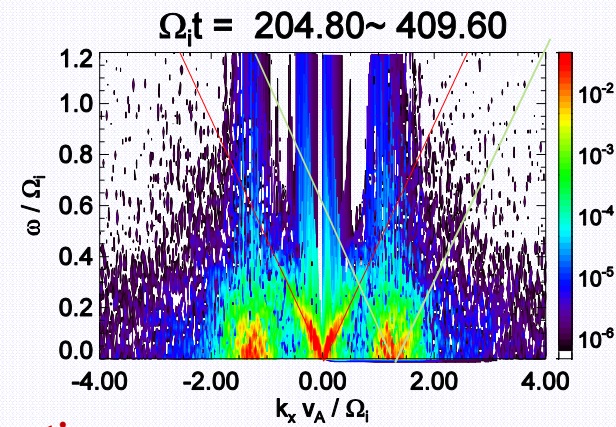


AIC's 2nd harmonic
(AIC^{2nd})

ω - k
of n_i

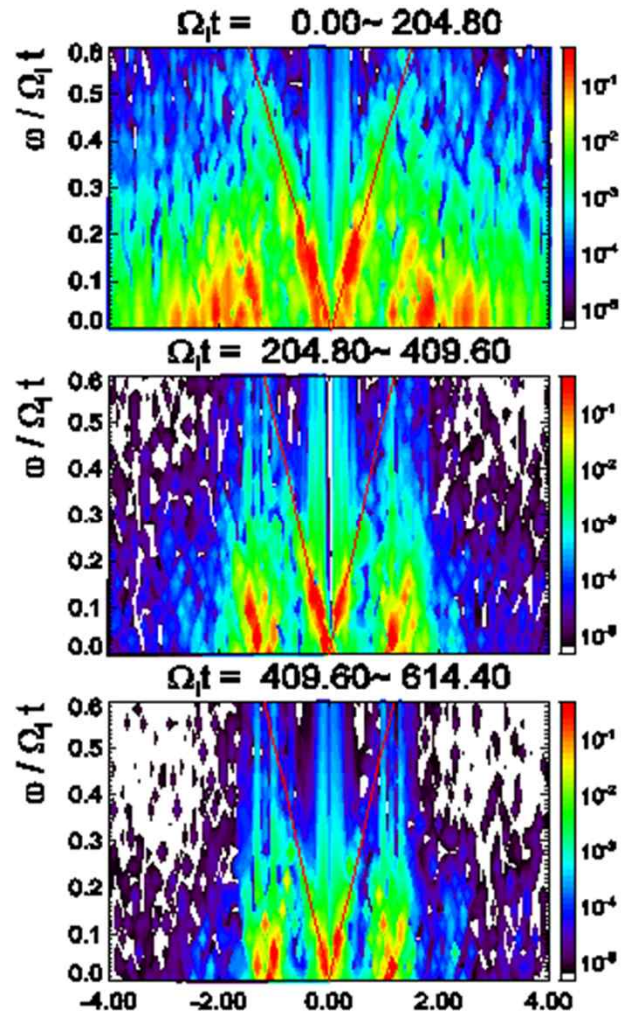


ion-acoustic
(IA)

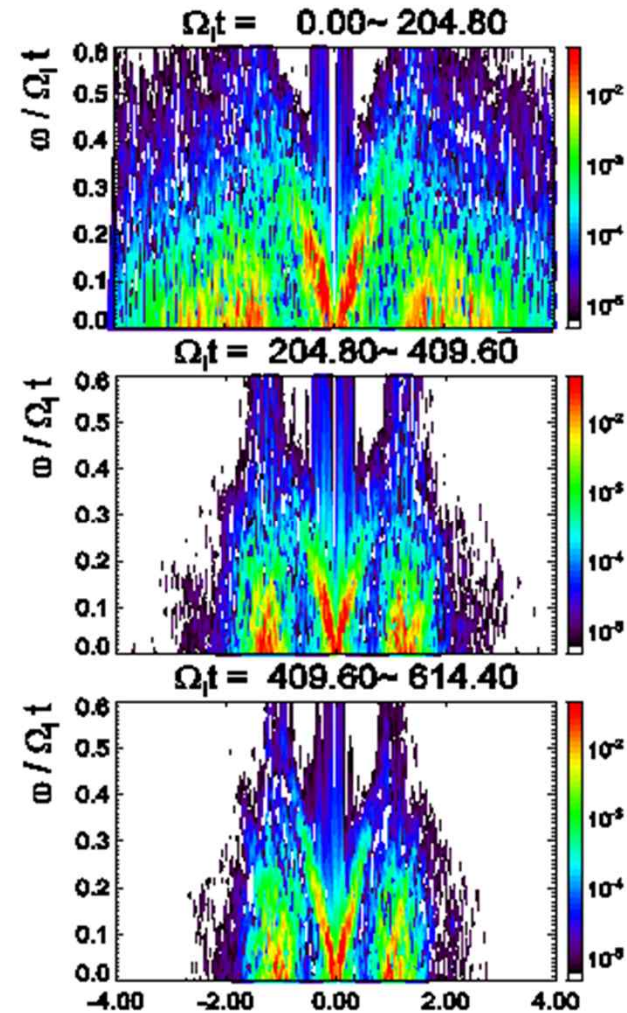


IA^{2nd} Mode for Different Number of Grids

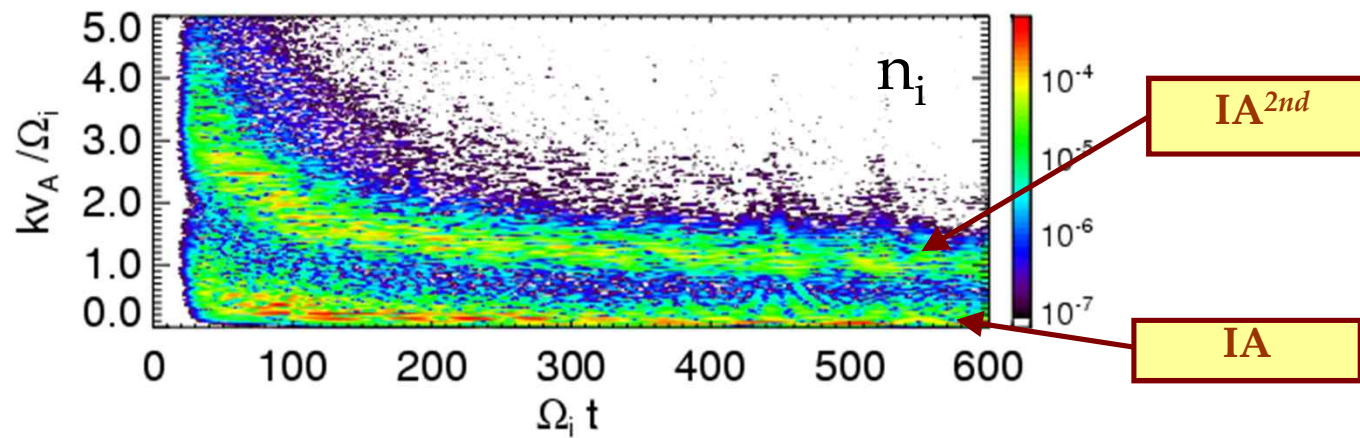
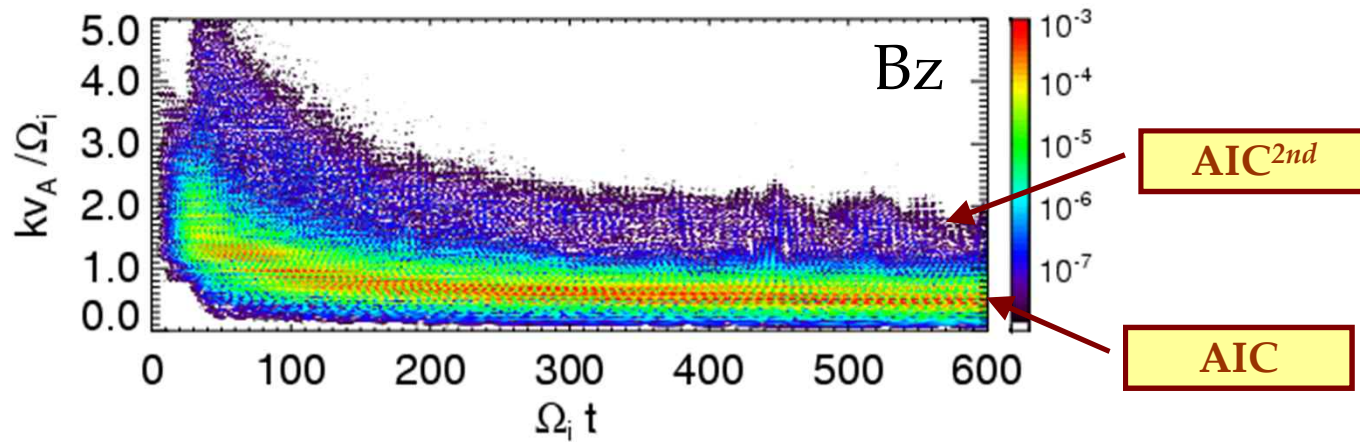
nx=4096



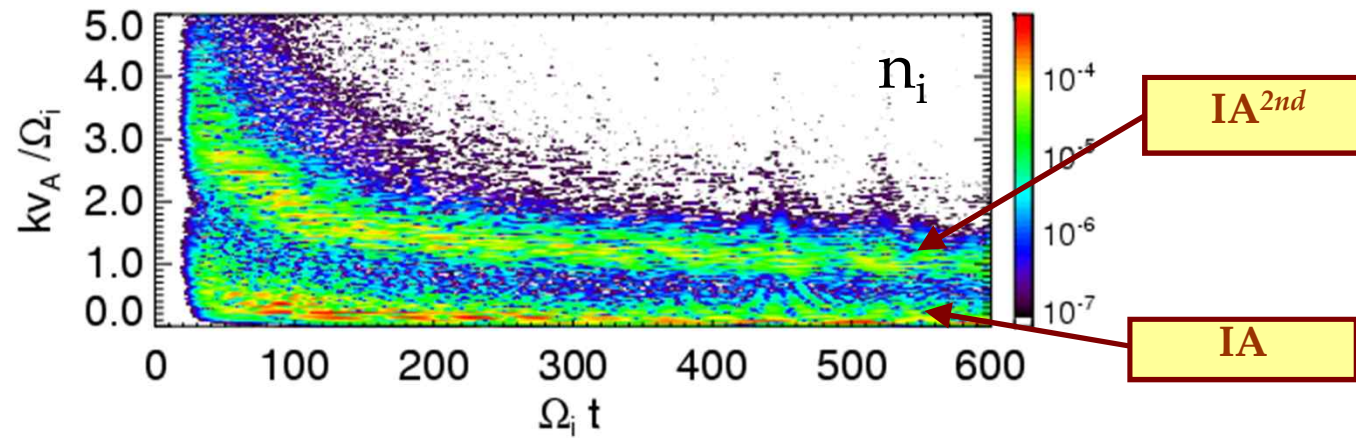
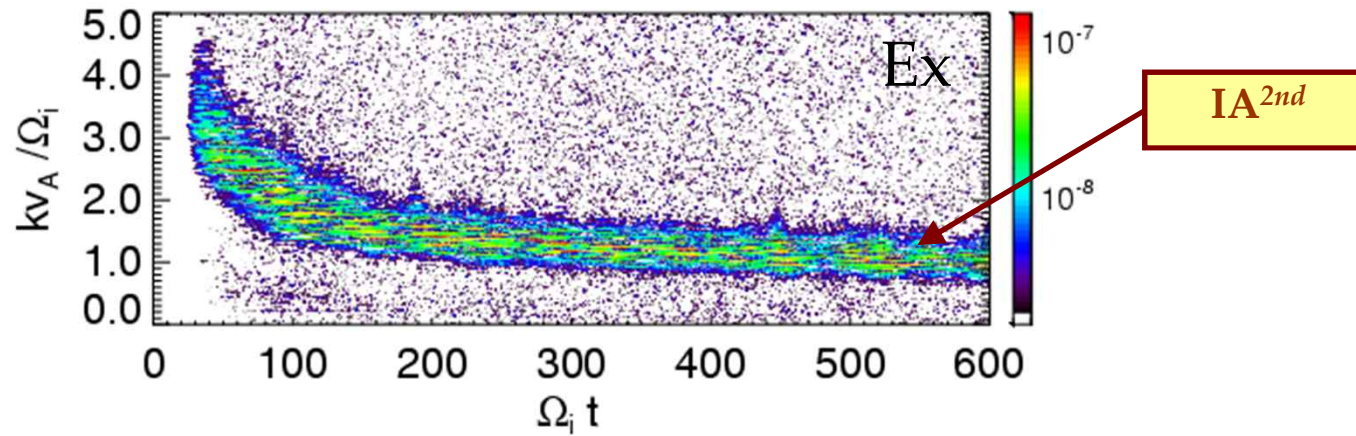
nx=16384



Inverse Cascade



Electrostatic Field and Ion Density



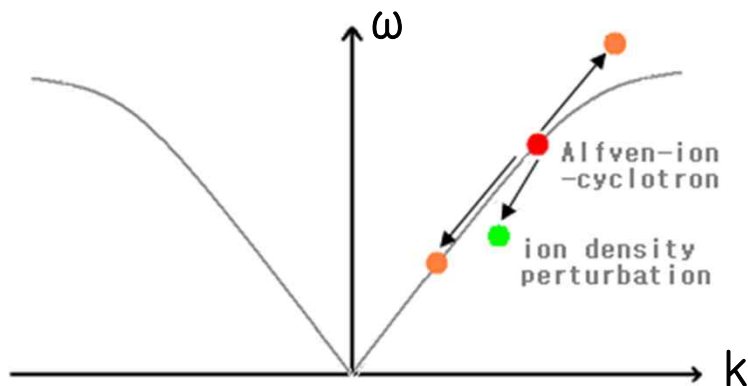
Parametric Instability

Alfvén waves (k_0, ω_0)

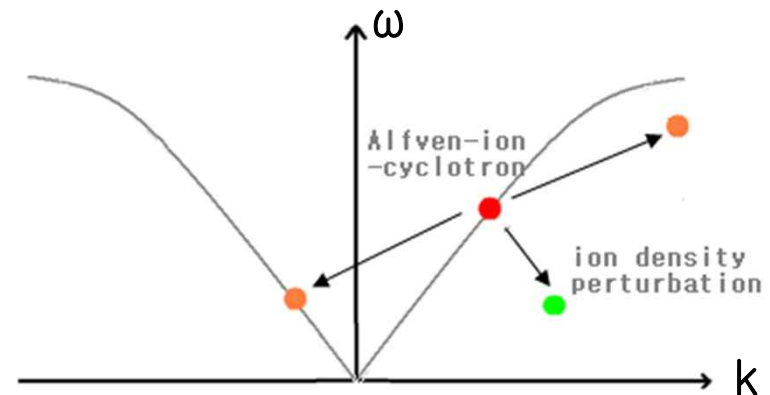
→ density mode (k, ω) + Alfvén waves ($k_0+k, \omega_0+\omega$) + Alfvén waves ($k_0-k, \omega_0-\omega$)

Polarization	Left-hand polarized	Right-hand polarized
Plasma beta (β)		
small β	modulational & decay	decay
large β	beat	modulational

modulational inst.



decay inst.



Governing Eqs.

$$\frac{\partial \rho}{\partial t} + \nabla \cdot [\rho \bar{V}] = 0$$

$$\frac{d\bar{V}}{dt} = \frac{1}{\rho} [\nabla \times \bar{B}] \times \bar{B} - \frac{1}{2\rho} \nabla P$$

$$\frac{\partial \bar{B}}{\partial t} = -\nabla \times \bar{E}$$

$$\bar{E} = -\bar{V} \times \bar{B} + \frac{1}{\rho} [\nabla \times \bar{B}] \times \bar{B} - \frac{1}{2\rho} \nabla P_e$$

Zeroth order solution

$$\overline{B}_\perp \equiv \begin{bmatrix} B_y \\ B_z \end{bmatrix} = \frac{1}{\sqrt{2}} \left[A_0 \exp i(k_0 x - \omega_0 t) \mathbf{e}_j + c.c. \right]$$

$$\text{where, } \mathbf{e}_j \equiv \frac{1}{\sqrt{2}} \left[\mathbf{e}_y + \hat{i} \cdot \mathbf{e}_z \right] \quad j = \begin{matrix} R \\ L \end{matrix}$$

$$\overline{V}_\perp = -\frac{k_0}{\omega_0} \overline{B}_\perp$$

$$k_0^2 = \frac{\omega_0^2}{1 \pm \omega_0} \quad \begin{matrix} R \\ L \end{matrix} \text{ polarization vector}$$

1st order solution

$$\vec{B}'_{\perp} \equiv \begin{pmatrix} B'_y \\ B'_z \end{pmatrix} = \frac{1}{\sqrt{2}} \left[A_+ \exp i(k_+ x - \omega_+ t) \vec{e}_j + c.c. + A_- \exp i(k_- x - \omega_- t) \vec{e}_j + c.c. \right]$$

$$k_{\pm} = k_0 \pm k, \quad \omega_{\pm} = \omega_0 \pm \omega$$

$$-\left[\omega^2 - k^2 C_s^2 \right] n_1 = -k^2 \left[A_+ A_0^* + A_-^* A_0 \right]$$

$$-\left[\omega_+^2 - k_+^2 (1 \pm \omega_+) \right] A_+ = \frac{1}{2} k_0 k_+ \left[1 \pm \omega_+ - \frac{\omega k_0}{k \omega_0} - \frac{\omega k_0 \omega_+}{k \omega_0 \omega_0} \right] n_1 A_0$$

$$-\left[\omega_-^2 - k_-^2 (1 \pm \omega_-) \right] A_-^* = \frac{1}{2} k_0 k_- \left[1 \pm \omega_- - \frac{\omega k_0}{k \omega_0} - \frac{\omega k_0 \omega_-}{k \omega_0 \omega_0} \right] n_1 A_0^*$$

[Terasawa et al., JGR(1986)]

Dispersion Eq. for Parametric Instability

$$L_-(L_+D+R_+B_+) + L_+L_-D = 0$$

$$X = \frac{\omega}{\Omega_i} \quad \text{and} \quad Y = \frac{kv_A}{\Omega_i}$$

$$L_{\pm} = Y_{\pm} - \frac{X_{\pm}}{\phi_{\pm}}$$

$$R_{\pm} = Y_{\pm} \left(X_0 - \frac{YX_0^2}{Y_0} + \frac{X_{\pm}}{\phi_{\pm}} \right) \frac{1}{2\phi_0}$$

$$B_{\pm} = \pm A \frac{X\phi_m (X\phi_{\pm}X_0^2 - Y_0\phi_0X_{\pm}^2)}{Y_0Y_{\pm}}$$

$$D = \phi_0\phi_+\phi_-\beta_e Y^2 - X^2 \left[\left(\frac{\delta B_{\perp}}{B_0} \right)^2 + \phi_0\phi_+\phi_-\left(1 - \beta_i \frac{Y^2}{X^2} \right) \right]$$

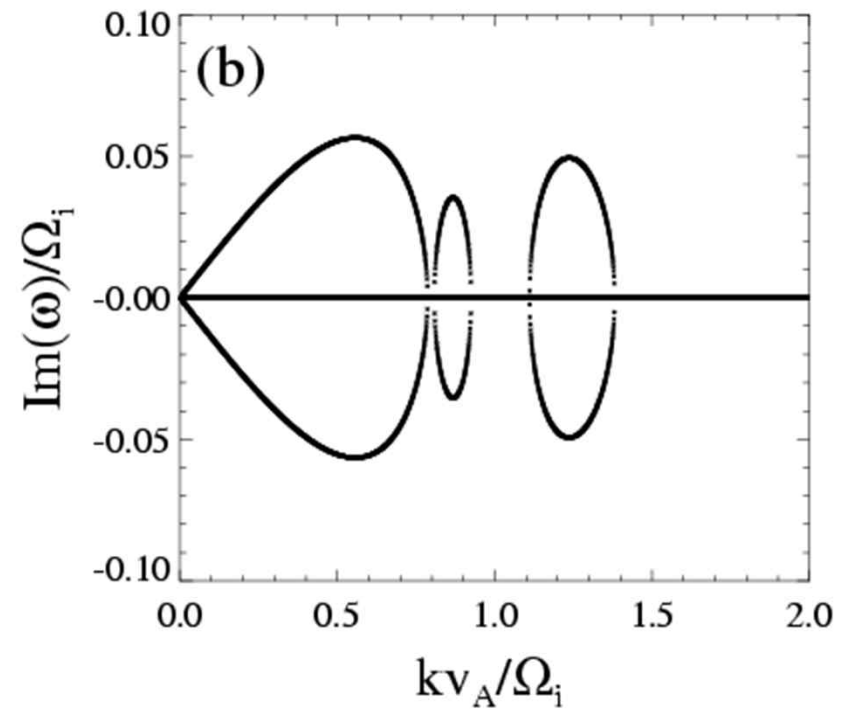
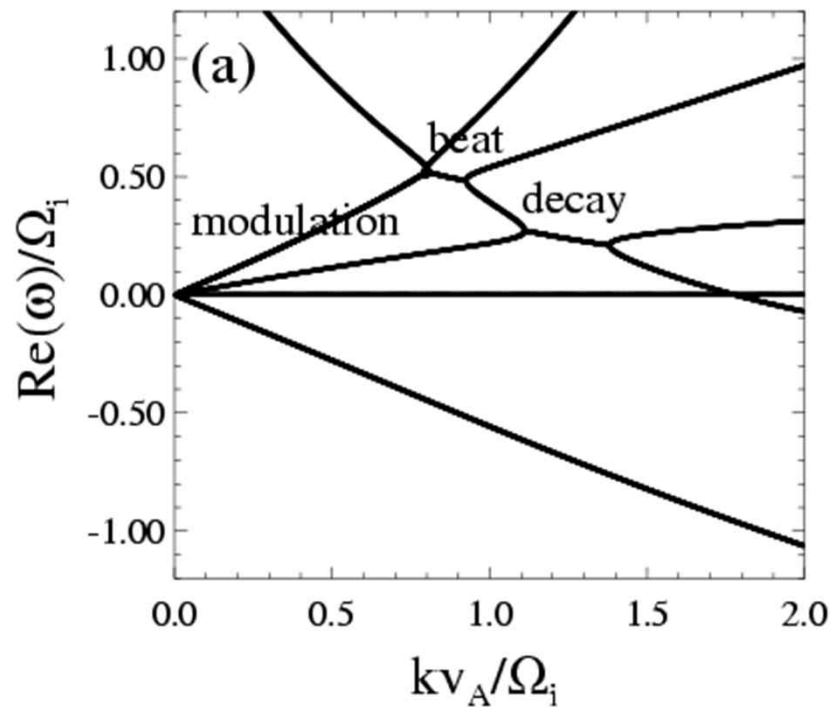
$$X_{\pm} = X_0 \pm X, \quad Y_{\pm} = Y_0 \pm Y, \quad \phi_0 = 1 - X_0, \quad \phi_{\pm} = 1 - X_{\pm}$$

[Araneda et al., JGR(2007)]

Numerical Solution

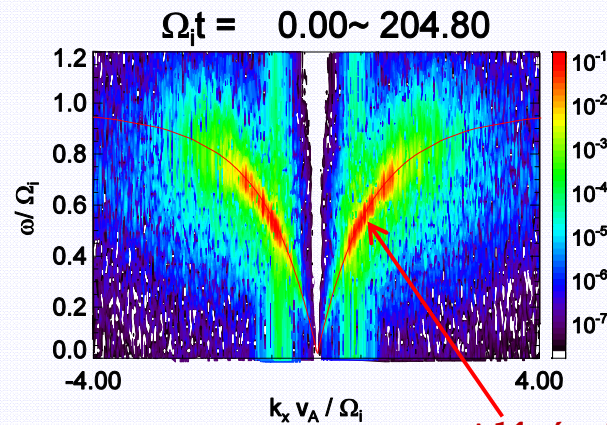
- Using the parameters from the simulation results

$$A = 0.2, \quad X_0 = 0.54, \quad Y_0 = 0.8, \quad \beta_e = 0.08, \quad \beta_i = 0.34$$

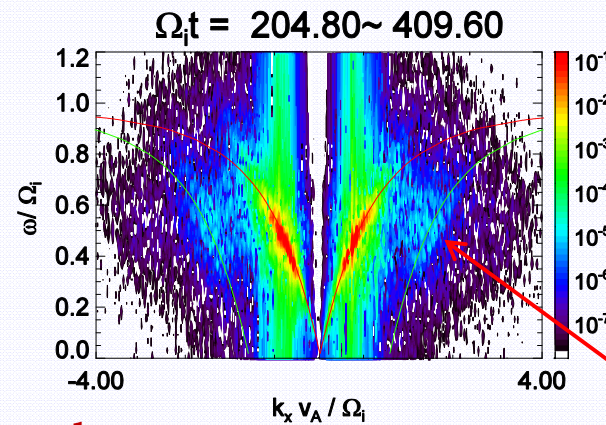


Excited Modes at Different Times

ω - k
of B_z

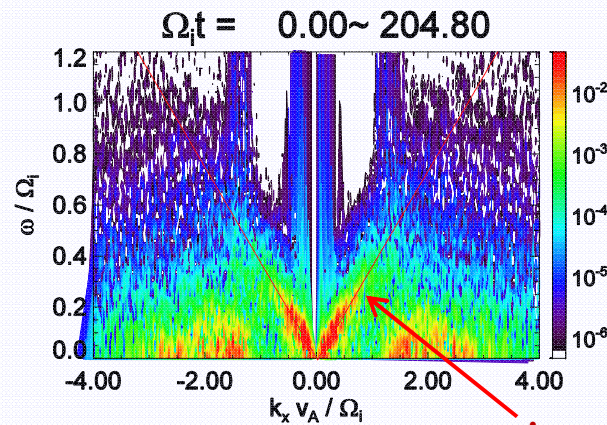


Alfvén-ion-cyclotron
(AIC)

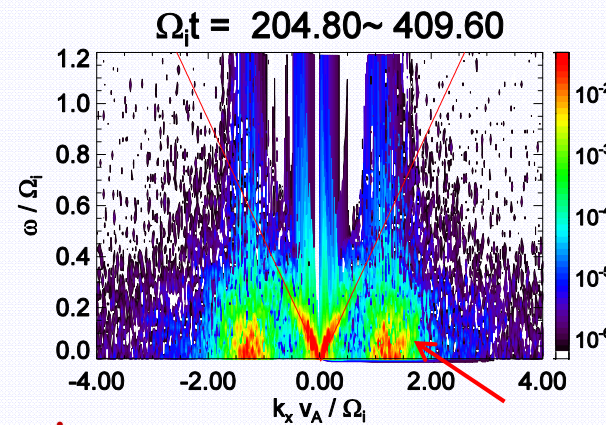


AIC's 2nd harmonic
(AIC^{2nd})

ω - k
of n_i



ion-acoustic
(IA)



IA's 2nd harmonic
(IA^{2nd})

Bicoherence Analysis

Three-wave interaction

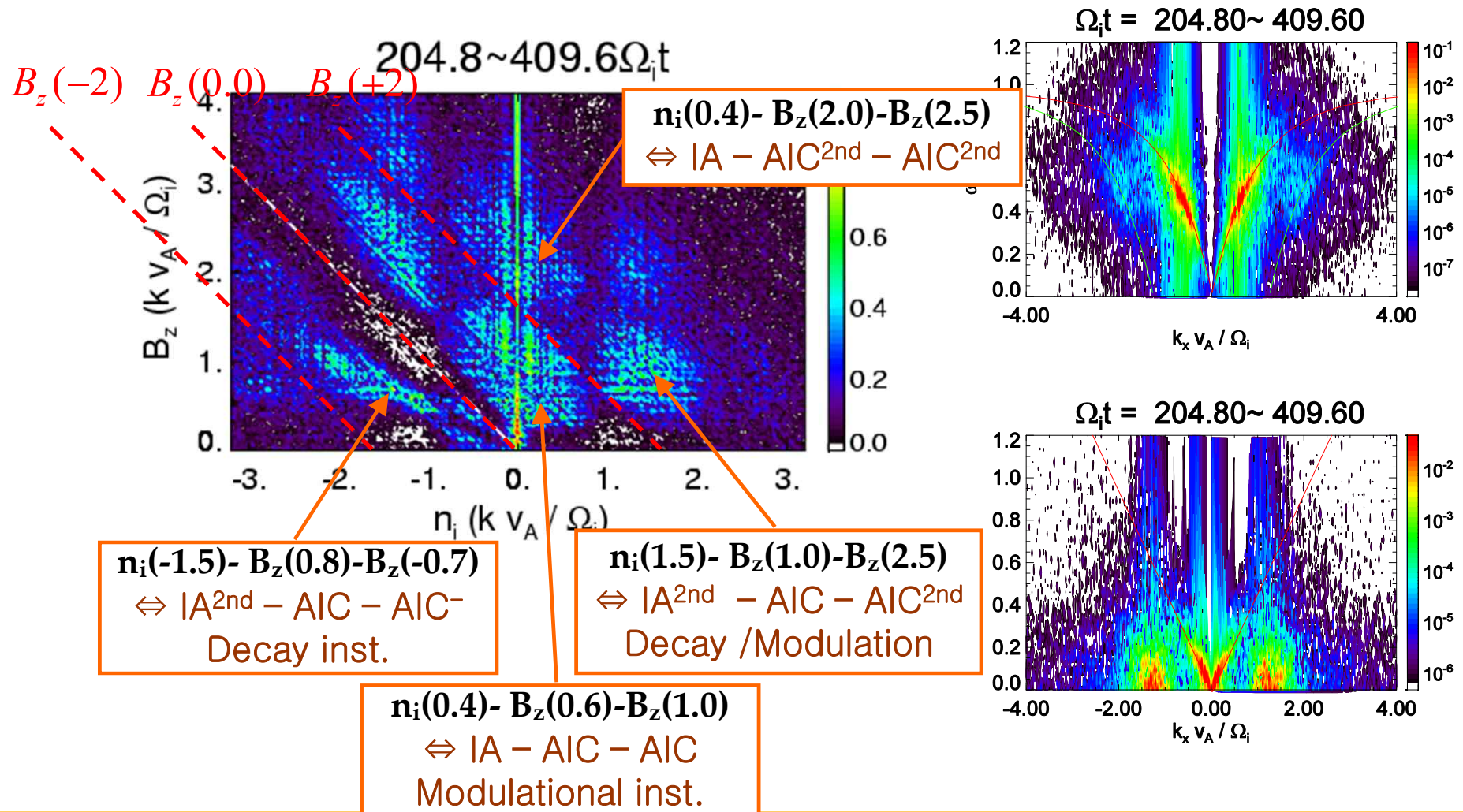
$$k_1 + k_2 = k_3$$

$$\omega_1 + \omega_2 = \omega_3$$

$$b(k_1, k_2) = \frac{|\langle f^{(1)}_{k_1} f^{(2)}_{k_2} f^{(3)}_{k_1+k_2} \rangle|}{\sqrt{\langle |f^{(1)}_{k_1} f^{(2)}_{k_2}|^2 \rangle \langle |f^{(3)}_{k_1+k_2}|^2 \rangle}}$$

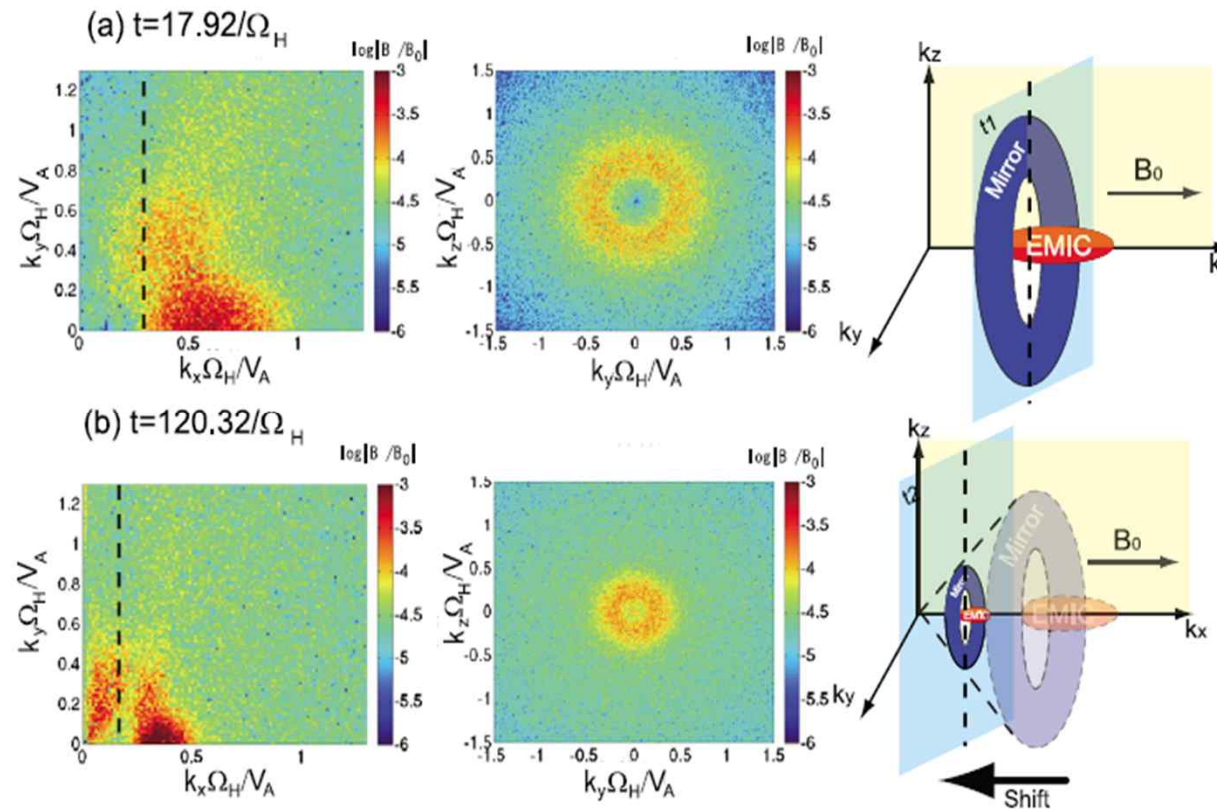
$$f^{(1)}_{k_1} + f^{(2)}_{k_2} \rightarrow f^{(3)}_{k_1+k_2} \quad \text{or} \quad f^{(3)}_{k_1+k_2} \rightarrow f^{(1)}_{k_1} + f^{(2)}_{k_2}$$

Bicoherence Spectrum



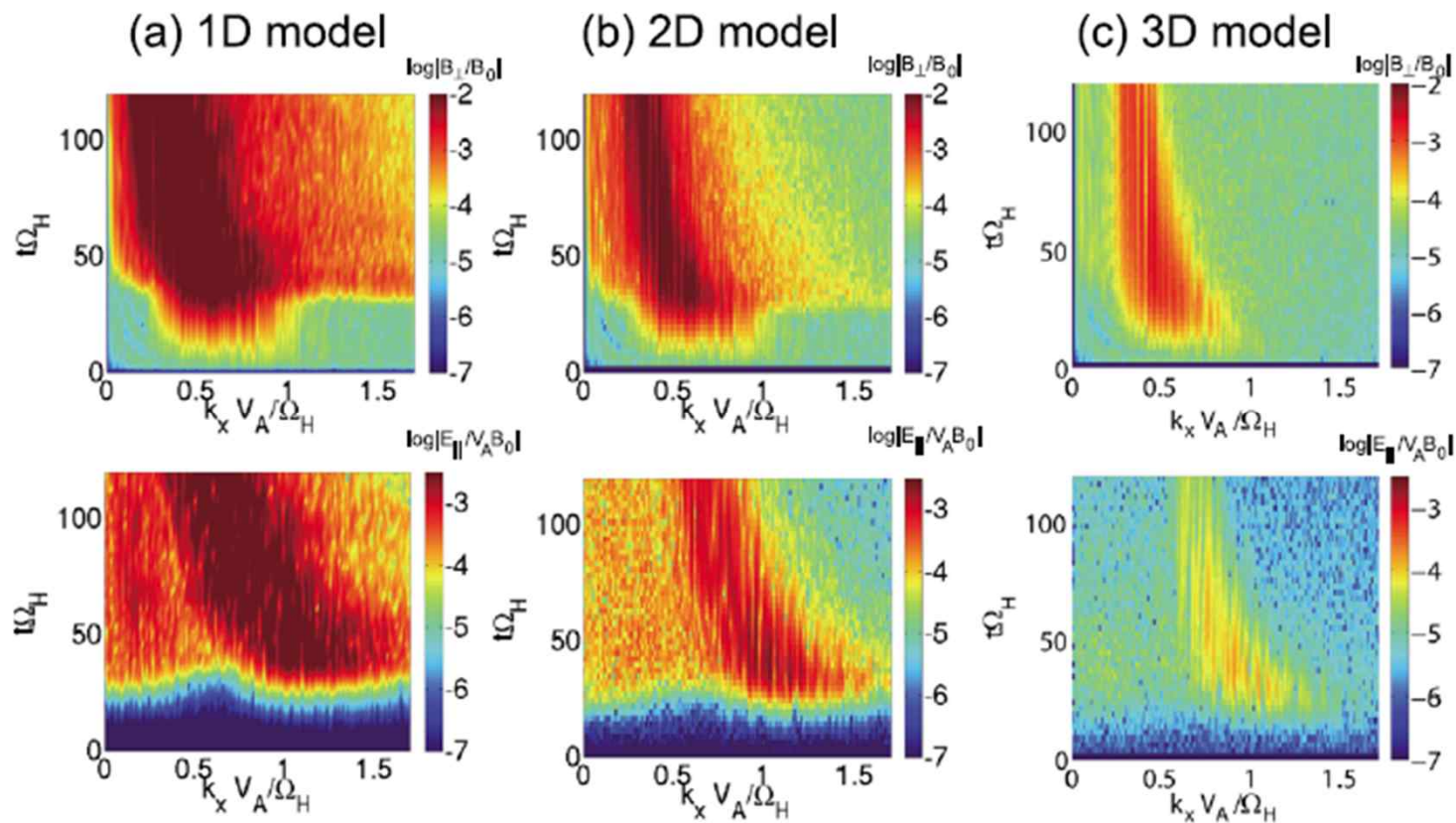
Anisotropic Temperature

- 3D Hybrid Simulation studies with $T_{\perp i} / T_{\parallel i} = 4$
; particle ions and fluid electrons
- EMIC & mirror modes are excited. [Shoji et al., JGR(2009)]



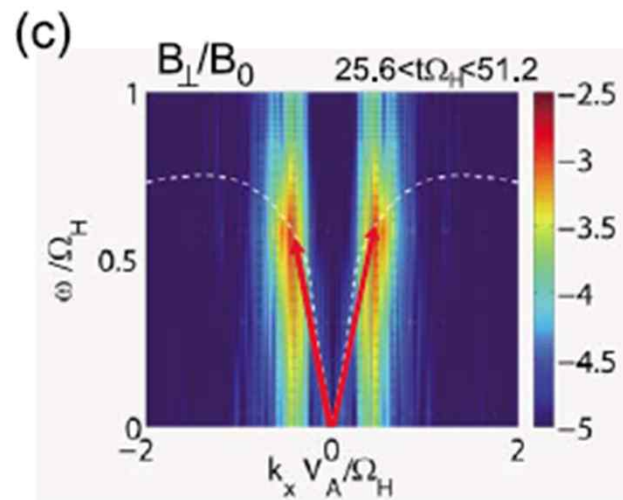
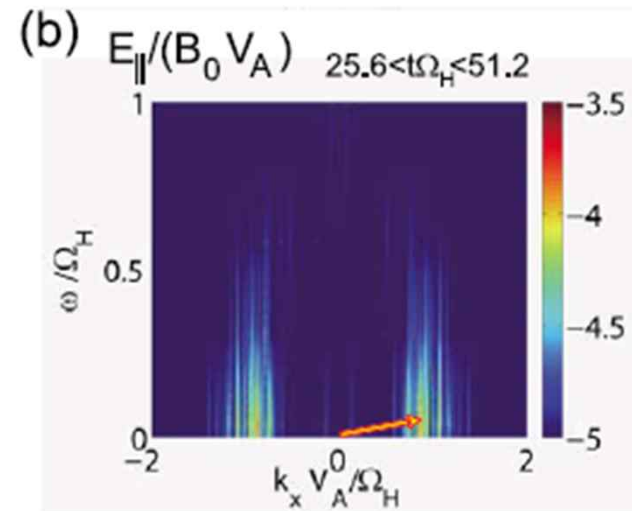
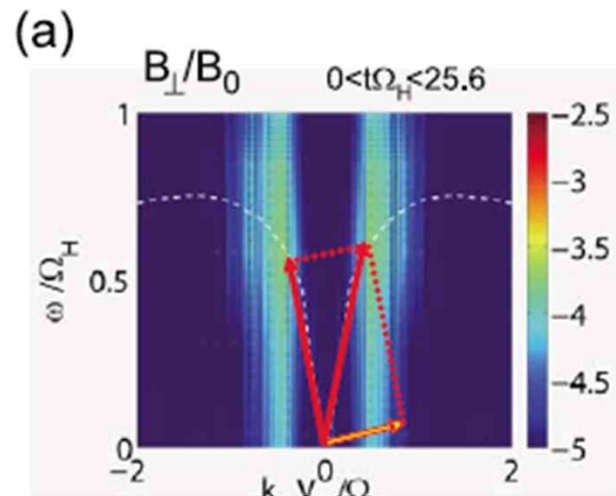
1~3D Hybrid Simulations

Simulation shows similar results regardless of dimension.



[Shoji et al., JGR(2009)].

Indication of 2nd harmonic IA mode



[Shoji et al.,
JGR(2009)].

Summary

- Alfvén-ion-cyclotron(AIC) waves and their turbulence are studied by using PIC simulations.
- The excited Alfvén ion-cyclotron(AIC) waves are unstable for the modulational and decay instability. By the modulational instability AIC waves are decomposed into an ion-acoustic(IA) wave and a lower k AIC wave. The decay instability brings AIC wave to be decomposed into the IA's 2nd harmonic mode(IA^{2nd}) and another AIC wave propagating in opposite direction.
- The 2nd harmonic mode of AIC waves are induced by nonlinear three-wave interaction between AIC and IA^{2nd} modes. The excited AIC harmonic mode decays into a lower-k AIC^{2nd} and IA waves.
- The inverse cascade takes place via the three-wave interaction of AIC waves. Modulational instability may be a key underlying mechanism for the inverse cascade process of the AIC turbulence.